

Closed-form approximations for the angle-of-arrival variance of plane and spherical waves propagating through homogeneous and isotropic turbulence

Yonghun Cheon and Andreas Muschinski

Department of Electrical and Computer Engineering, University of Massachusetts, Amherst, 151 Holdsworth Way, Amherst, Massachusetts 01003-9284

Received June 9, 2006; accepted July 28, 2006;
posted September 5, 2006 (Doc. ID 71779); published January 10, 2007

The calculation of the aperture-averaged angle-of-arrival variance, observed with a telescope with a circular aperture, of a plane or spherical wave propagating through homogeneous and isotropic turbulence is one of the classical problems in the theory of wave propagation through random media. We present and discuss approximate closed-form solutions on the basis of the Rytov approximation. For both plane and spherical waves, the accuracy of the approximations is better than 0.25% for all ratios of aperture diameter and Fresnel length.

© 2007 Optical Society of America

OCIS codes: 010.1300, 010.1330, 010.7350.

1. INTRODUCTION

Angle-of-arrival (AOA) fluctuations of optical waves propagating through random media have been studied for various purposes, such as for retrieving characteristics of atmospheric turbulence, studying and mitigating errors in free-space optical communication, and overcoming limitations for ground-based astronomical observations.

Predicting the AOA variance, $\langle \bar{\theta}^2 \rangle$, observed with a telescope with a circular aperture of diameter D , of plane or spherical waves propagating along a path of length L through a turbulent refractive index field characterized by the refractive index structure parameter C_n^2 , is a classical problem in the theory of wave propagation through random media. It is known¹⁻³ that the AOA variances for plane and spherical waves propagating through homogeneous and locally isotropic inertial subrange turbulence are given by

$$\langle \bar{\theta}^2 \rangle_p = \gamma_p(q) C_n^2 L D^{-1/3}, \quad (1)$$

$$\langle \bar{\theta}^2 \rangle_s = \gamma_s(q) C_n^2 L D^{-1/3}, \quad (2)$$

respectively, where the dimensionless coefficients $\gamma_p(q)$ and $\gamma_s(q)$ are functions of the ‘‘Fresnel number’’ q , the ratio between the aperture diameter and the Fresnel length

$$q = \frac{D}{f}, \quad (3)$$

where

$$f = \sqrt{\lambda L} \quad (4)$$

is the Fresnel length, and λ , is the wavelength of the unperturbed wave. Only little seems to be known, however,

about the details of $\gamma_p(q)$ and $\gamma_s(q)$, in particular, in the important intermediate range where q is of order 1.

Tatarskii^{1,2} has shown that for an interferometer, the AOA variance can be expressed in terms of the phase structure function and baseline distance and that for an observation with a telescope, by considering a diffracted wave incident upon the aperture without a lens, the AOA variance can be expressed as a weighted aperture average of the derivative of the phase structure function. Tatarskii expressed the AOA variance in closed form for the asymptotic cases $q \gg 1$ and $q \ll 1$, and he showed that $\langle \bar{\theta}^2 \rangle$ for large-aperture telescopes ($q \gg 1$) is twice the value of $\langle \bar{\theta}^2 \rangle$ for point receivers ($q \ll 1$). It was pointed out early by Gurvich and Kallistratova⁴ that for AOA fluctuations, in contrast to log-amplitude fluctuations, weak-scattering theory (based on the Rytov approximation) remains valid far into the strong-scattering regime. Churnside and Lataitis⁵ and Churnside⁶ studied, based on geometrical optics, AOA fluctuations of a laser beam and compared their theoretical results with field observations.

There have been attempts to obtain the AOA variance in a more compact form. Tofsted⁷ studied how AOA variances for Gaussian and uniform-intensity beams are affected by the inner and outer scales of turbulence. The author presented the AOA variance as a double integral over the propagation path and the spatial wavenumber of the refractive index fluctuations, which he then condensed, by means of a curve-fitting approximation, into a single integral over the propagation path. Conan *et al.*⁸ expressed the AOA spatial covariance and the variance as a convergent series using the Mellin transforms. The AOA variance can be obtained in a closed form, however, by means of a simple and analytical approximation, as we will show in this paper.

Recently, Wheelon³ and Andrews and Phillips⁹ investi-

gated AOA fluctuations based on geometrical optics for plane and spherical waves and presented closed-form solutions of AOA variances including the inner and outer scales of turbulence by approximating the phase structure function. These solutions, however, are valid only for the asymptotic cases $q \gg 1$ and $q \ll 1$.

Our motivation for developing closed-form AOA variances for plane and spherical waves propagating through fully developed, homogeneous, and locally isotropic turbulence is to obtain a deeper understanding and to reduce the numerical computation time for AOA variances. While previous works¹⁻³ have provided asymptotic solutions of AOA variances for $q \gg 1$ and $q \ll 1$, there appears to be a lack of analytical understanding of the intermediate regime $q \approx 1$, that is, the behavior of $\langle \bar{\theta}^2 \rangle$ for an aperture diameter comparable to the Fresnel length. Because the intermediate regime is of great practical relevance for many applications, there is a need for closed-form solutions or approximations of $\gamma_p(q)$ and $\gamma_s(q)$ for $q \approx 1$. To fill this gap is the main purpose of this paper.

This paper is organized as follows. In Section 2, we begin with the AOA variance, $\langle \bar{\theta}^2 \rangle$, for plane and spherical waves observed by a circular-aperture telescope. We show that the Airy weighting function can be approximated by a Gaussian weighting function with an analytically calibrated width parameter β , and the double integral of $\langle \bar{\theta}^2 \rangle$ can be solved in closed form. In Section 3, we discuss the validity of the Gaussian approximation of the Airy function and the accuracy of the closed-form approximation of $\langle \bar{\theta}^2 \rangle$ in terms of q . We compare our results with previously known analytical and computational results. A summary and conclusions are given in Section 4.

2. THEORETICAL ANALYSIS

For both plane and spherical waves propagating through fully developed, homogeneous, and locally isotropic turbulence, the aperture-averaged AOA variance can be presented in the form^{4,10}

$$\langle \bar{\theta}^2 \rangle = \pi L \int_0^\infty d\kappa \int_0^1 du \kappa^3 \Phi_n(\kappa) h(\kappa, u), \quad (5)$$

where u is the normalized path coordinate (such that $u=0$ at the source and $u=1$ at the receiving aperture), κ is the magnitude of the wave vector transverse to the propagation path, $\Phi_n(\kappa)$ is the local, three-dimensional wavenumber spectrum of the refractive index fluctuations, and $h(\kappa, u)$ is a weighting function, which is

$$h_p(\kappa) = \left[1 + \frac{2\pi}{(\kappa f)^2} \sin \frac{(\kappa f)^2}{2\pi} \right] A(a\kappa) \quad (6)$$

for plane waves and

$$h_s(\kappa, u) = \left[1 + \cos \frac{(\kappa f)^2 u(1-u)}{2\pi} \right] u^2 A(a\kappa u) \quad (7)$$

for spherical waves. Here, $a=D/2$ is the radius of the aperture, and

$$A(x) = \left(\frac{2J_1(x)}{x} \right)^2 \quad (8)$$

is the Airy function, which comes from averaging over a circular aperture, with $J_1(x)$ as the first-order Bessel function. Note that $h_p(\kappa)$, the weighting function for the plane wave, does not vary with u , in contrast to $h_s(\kappa, u)$, the weighting function for the spherical wave, which does vary with u .

For homogeneous and locally isotropic turbulence, the three-dimensional refractive index spectrum in the inertial subrange is (see p. 48 in Ref. 1):

$$\Phi_n(\kappa) = \frac{\Gamma(8/3) \sin(\pi/3)}{4\pi^2} C_n^2 \kappa^{-11/3}. \quad (9)$$

A. Approximating the Airy Function by a Gaussian Function

The aperture-averaged AOA variance, $\langle \bar{\theta}^2 \rangle$ in Eq. (5), is a weighted integral of the Airy function $A(a\kappa)$ and therefore should not be too sensitive to the details of $A(a\kappa)$. Because $A(0)=1$ and because $A(a\kappa)$ drops fairly rapidly to zero at wavenumbers comparable to a^{-1} , $A(a\kappa)$ can be quite well approximated by a Gaussian function,

$$A(a\kappa) \approx \exp[-(\beta a\kappa)^2], \quad (10)$$

as illustrated in Fig. 1. Haddon and Vilar¹¹ used this approximation for the case of scintillation. Their value of β is different from our value, and the authors did not describe in detail how they calibrated their β , however.

For plane waves, we insert $h_p(\kappa)$ given in Eq. (6), approximate $A(a\kappa)$ with the Gaussian function, and obtain

$$\langle \bar{\theta}^2 \rangle_g = \pi^2 L \int_0^1 du \int_0^\infty d\kappa \kappa^3 \Phi_n(\kappa) \left[1 + \frac{2\pi}{(\kappa f)^2} \sin \frac{(\kappa f)^2}{2\pi} \right] \times \exp[-(\beta a\kappa)^2]. \quad (11)$$

Now, we calibrate the width parameter β such that $\langle \bar{\theta}^2 \rangle_g$

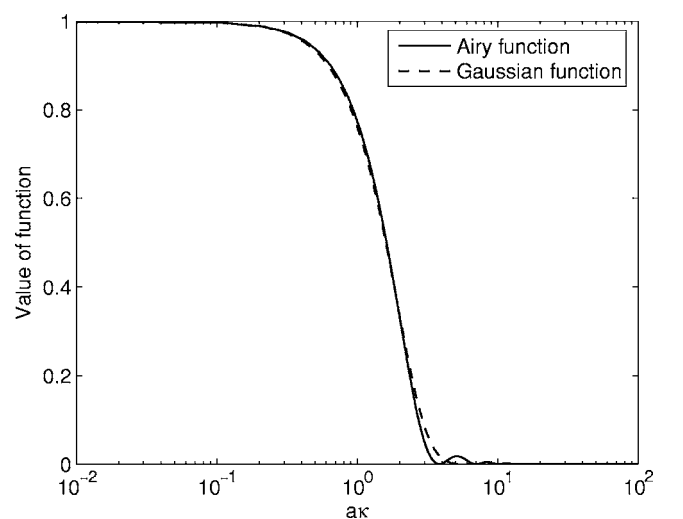


Fig. 1. Airy function and the Gaussian function with $\beta = 0.5216$. The solid curve is the Airy function and the dashed curve is the Gaussian function.

$= \langle \bar{\theta}^2 \rangle_{GO}$, where $\langle \bar{\theta}^2 \rangle_{GO}$ is the aperture-averaged AOA variance with the Airy weighting function in the geometrical-optics (GO) limit. In the GO limit, we have $\kappa f \ll 1$ for all κ that contribute significantly to the integral for $\langle \bar{\theta}^2 \rangle$, such that $h_p(\kappa) = 2A(a\kappa)$. Inserting Eqs. (8) and (9) gives

$$\begin{aligned} \langle \bar{\theta}^2 \rangle_{GO} &= \sqrt{3} \Gamma\left(\frac{8}{3}\right) C_n^2 a^{-2} \int_0^\infty d\kappa \kappa^{-8/3} J_1^2(a\kappa) \\ &= C_n^2 L \frac{1296 \sqrt{3} [\Gamma(8/3)]^2 \Gamma(1/6)}{2^{8/3} 1375 [\Gamma(5/6)]^3} a^{-1/3}, \end{aligned} \quad (12)$$

where we have used Eq. (A1). On the other hand, the aperture-averaged AOA variance with the Gaussian weighting function in the GO limits is

$$\begin{aligned} \langle \bar{\theta}^2 \rangle_g &= \frac{\sqrt{3}}{4} \Gamma\left(\frac{8}{3}\right) C_n^2 L \int_0^\infty d\kappa \kappa^{-2/3} \exp[-(\beta a \kappa)^2] \\ &= C_n^2 L \frac{\sqrt{3}}{8} \Gamma\left(\frac{8}{3}\right) \Gamma\left(\frac{1}{6}\right) \beta^{-1/3} a^{-1/3}, \end{aligned} \quad (13)$$

where we have used Eq. (A2). We obtain β by equating Eq. (12) with Eq. (13):

$$\beta = \frac{5^6 11^3 [\Gamma(5/6)]^9}{2^{16} 3^6 [\Gamma(2/3)]^3} = 0.5216. \quad (14)$$

For spherical waves, we can calibrate correspondingly, and we obtain the same result.

B. Plane Wave

Now, having β properly calibrated, we evaluate the Gaussian-approximated, aperture-averaged AOA variance for a plane wave,

$$\begin{aligned} \langle \bar{\theta}^2 \rangle_p &= \frac{\sqrt{3}}{8} \Gamma\left(\frac{8}{3}\right) C_n^2 L \int_0^\infty d\kappa \kappa^{-2/3} \left[1 + \frac{2\pi}{(\kappa f)^2} \sin\left(\frac{\kappa f}{2\pi}\right)^2 \right] \\ &\quad \times \exp[-(\beta a \kappa)^2]. \end{aligned} \quad (15)$$

By means of Eqs. (A2) and (A3), the closed-form aperture-averaged AOA variance for the plane wave is

$$\langle \bar{\theta}^2 \rangle_p = \gamma_p(q) C_n^2 L D^{-1/3}, \quad (16)$$

where

$$\begin{aligned} \gamma_p(q) &= \frac{\sqrt{3}}{16} \Gamma\left(\frac{1}{6}\right) \Gamma\left(\frac{8}{3}\right) \left(\frac{\beta}{2}\right)^{-1/3} \\ &\quad \times \left\{ 1 + \frac{6}{5} \left(\frac{\pi}{2}\right)^{1/6} \beta^{1/3} q^{1/3} \left[1 + \frac{\pi^2}{4} \beta^4 q^4 \right]^{5/12} \right. \\ &\quad \left. \times \sin\left[\frac{5}{6} \arctan\left(\frac{2}{\pi \beta^2 q^2}\right) \right] \right\}. \end{aligned} \quad (17)$$

C. Spherical Wave

The Gaussian-approximated, aperture-averaged AOA variance for a spherical wave is

$$\begin{aligned} \langle \bar{\theta}^2 \rangle_s &= \frac{\sqrt{3}}{8} \Gamma\left(\frac{8}{3}\right) C_n^2 L \int_0^1 du u^2 \int_0^\infty d\kappa \kappa^{-2/3} \\ &\quad \times \left[1 + \cos\left(\frac{(\kappa f)^2 u(1-u)}{2\pi}\right) \right] \exp[-(\beta a \kappa u)^2]. \end{aligned} \quad (18)$$

We can evaluate Eq. (18) by dividing the integral into two integrals. The first integral is, by means of Eq. (A2),

$$\begin{aligned} I_1 &= \int_0^1 du u^2 \int_0^\infty d\kappa \kappa^{-2/3} \exp[-(\beta a \kappa u)^2] \\ &= \frac{3}{8} \frac{1}{2} \Gamma\left(\frac{1}{6}\right) \beta^{-1/3} a^{-1/3}. \end{aligned} \quad (19)$$

The second integral is, after expressing the cosine function in terms of the exponential functions with imaginary arguments,

$$\begin{aligned} I_2 &= \int_0^1 du u^2 \int_0^\infty d\kappa \kappa^{-2/3} \cos\left(\frac{(\kappa f)^2 u(1-u)}{2\pi}\right) \exp[-(\beta a \kappa u)^2] \\ &= \frac{1}{4} \Gamma\left(\frac{1}{6}\right) \beta^{-1/3} a^{-1/3} \int_0^1 du u^2 [(C_1 u^2 - C_2 u)^{-1/6} + (C_3 u^2 \\ &\quad + C_2 u)^{-1/6}] = I_{21} + I_{22}, \end{aligned} \quad (20)$$

where we have used Eqs. (A2) and (A4). I_{21} and I_{22} are

$$I_{21} = \frac{1}{4} \Gamma\left(\frac{1}{6}\right) (\beta a)^{-1/3} \frac{6}{17} (-C_2)^{-1/6} {}_2F_1\left(\frac{1}{6}, \frac{17}{6}; \frac{23}{6}; \frac{C_1}{C_2}\right), \quad (21)$$

$$I_{22} = \frac{1}{4} \Gamma\left(\frac{1}{6}\right) (\beta a)^{-1/3} \frac{6}{17} C_2^{-1/6} {}_2F_1\left(\frac{1}{6}, \frac{17}{6}; \frac{23}{6}; -\frac{C_3}{C_2}\right), \quad (22)$$

where

$$C_1 = 1 + \frac{if^2}{2\pi\beta^2 a^2} = 1 + C_2, \quad (23)$$

$$C_2 = \frac{if^2}{2\pi\beta^2 a^2} = \frac{2i}{\pi\beta^2 q^2}, \quad (24)$$

$$C_3 = 1 - \frac{if^2}{2\pi\beta^2 a^2} = 1 - C_2, \quad (25)$$

with $i = \sqrt{-1}$. C_2 is purely imaginary. Since $(C_2)^{-1/6} = [(-C_2)^{-1/6}]^*$ and $C_1/C_2 = (-C_3/C_2)^*$, I_{22} is the complex conjugate of I_{21} (* stands for the complex conjugate). Thus, we find

$$\langle \bar{\theta}^2 \rangle_s = \gamma_s(q) C_n^2 L D^{-1/3}, \quad (26)$$

where

$$\begin{aligned} \gamma_s(q) = & \frac{3\sqrt{3}}{816} \Gamma\left(\frac{1}{6}\right) \Gamma\left(\frac{8}{3}\right) \left(\frac{\beta}{2}\right)^{-1/3} \\ & \times \left[1 + \frac{68}{173} \operatorname{Re} \left\{ \left(-\frac{2i}{\pi\beta^2 q^2} \right)^{-1/6} \right. \right. \\ & \left. \left. \times {}_2F_1\left(\frac{1}{6}, \frac{17}{6}; \frac{23}{6}; 1 - \frac{i\pi\beta^2 q^2}{2}\right) \right\} \right]. \end{aligned} \quad (27)$$

Re stands for the real part. We can express $\gamma_s(q)$ as a summation form by means of Eqs. (A5) and (A6):

$$\begin{aligned} \gamma_s(q) = & \frac{3\sqrt{3}}{816} \Gamma\left(\frac{1}{6}\right) \Gamma\left(\frac{8}{3}\right) \left(\frac{\beta}{2}\right)^{-1/3} \\ & \times \left[1 + \frac{68}{173} \left(\frac{2}{\pi\beta^2 q^2}\right)^{-1/6} (\gamma_{s1} + \gamma_{s2}) \right], \end{aligned} \quad (28)$$

where

$$\begin{aligned} \gamma_{s1} = & \frac{\Gamma(23/6)\Gamma(5/6)}{\Gamma(22/6)} \left[\cos\left(\frac{\pi}{12}\right) \sum_{n=0}^{\infty} \binom{17}{2n} \frac{(-1)^n (\pi\beta^2 q^2/2)^{2n}}{(2n)!} \right. \\ & \left. - \sin\left(\frac{\pi}{12}\right) \sum_{n=0}^{\infty} \binom{17}{2n+1} \frac{(-1)^{n+2} (\pi\beta^2 q^2/2)^{2n+1}}{(2n+1)!} \right], \quad (29) \\ \gamma_{s2} = & - \left(\frac{\pi\beta^2 q^2}{2}\right)^{5/6} \frac{\Gamma(23/6)\Gamma(-5/6)}{\Gamma(1/6)\Gamma(17/6)} \\ & \times \sum_{n=0}^{\infty} \frac{(22/6)_{2n+1} (1)_{2n+1}}{(11/6)_{2n+1}} \frac{(-1)^{n+2} (\pi\beta^2 q^2/2)^{2n+1}}{(2n+1)!}. \end{aligned} \quad (30)$$

3. DISCUSSION

In Section 2, by introducing the Gaussian approximation of the Airy function with a properly calibrated width parameter β , we obtained a closed-form approximation for the variance $\langle \bar{\theta}^2 \rangle$ of the aperture-averaged AOA fluctuations. In the following, the validity for the Gaussian approximation of the Airy function is discussed. The accuracy of our closed-form approximation of $\langle \bar{\theta}^2 \rangle$ is evaluated in terms of q ranging from zero (point receiver) to infinity (large-aperture receiver). Finally, the ratio of $\langle \bar{\theta}^2 \rangle$ between spherical and plane waves is discussed.

A. Gaussian Approximation of the Airy Function

Figure 1 shows the Airy function, $A(a\kappa)$ and the calibrated Gaussian function. The Airy function drops from 1 rapidly to its first null at $a\kappa=3.83$, reaches its first secondary maximum of 0.0175 at $a\kappa=5.13$, and it has its second null at $a\kappa=7.02$. The Airy function plays the role of a low-pass filter, such that inhomogeneities smaller than the aperture diameter contribute only little to the aperture-averaged AOA variance. The calibrated Gaussian function agrees well with the Airy function. The discrepancy between the Airy function and the Gaussian function is shown in Fig. 2. The largest discrepancy occurs between $a\kappa=0.5$ and $a\kappa=7$, an interval that contains

the first null and the first sidelobe of the Airy function. We will see that replacing the Airy function with the calibrated Gaussian function leads to an error of less than 1% in $\langle \bar{\theta}^2 \rangle$, both in the plane-wave case and the spherical-wave case.

B. Aperture-Averaged Angle-of-Arrival Variance for the Plane Wave

Figure 3 shows three curves of $\gamma_p(q)$: a numerical solution of the integral (5) with the exact plane wave weighting function $h_p(\kappa)$ given in Eq. (6), our closed-form approximation (with the Gaussian weighting function) as given in Eq. (17), and the asymptotic fit as given later in Eq. (34). Figure 4 shows the difference between the exact numerical solution and the closed-form approximation of $\langle \bar{\theta}^2 \rangle$ for plane and spherical waves, respectively. The difference is largest for q in between 0.3 and 6 and the maximum value of the difference is 0.22% at $q \approx 1.1$, which is probably negligible for all practical applications.

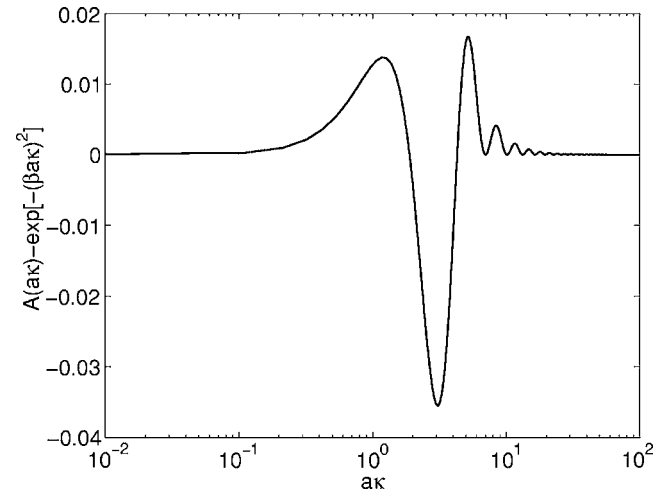


Fig. 2. Discrepancy between the Airy function and the Gaussian function, $A(a\kappa) - \exp[-(\beta a\kappa)^2]$ with $\beta=0.5216$.

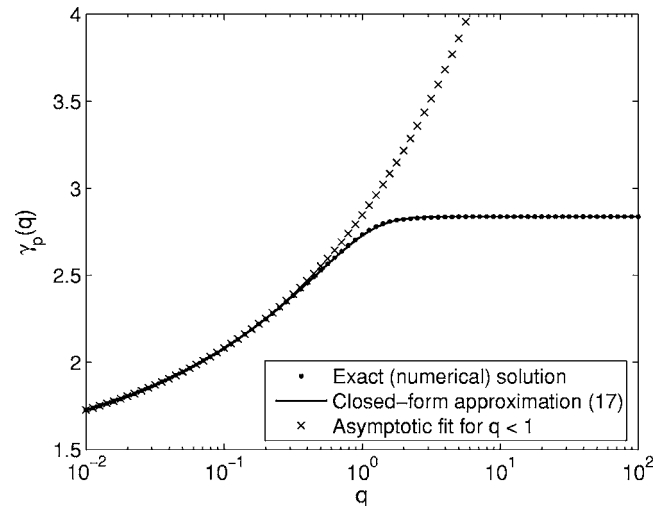


Fig. 3. Aperture-averaged AOA variance, normalized by $C^2LD^{-1/3}$, versus q for a plane wave. The dots are the exact (numerical) solution; the solid curve is the closed-form approximation (17), and the crosses are the asymptotic fit for $q < 1$.

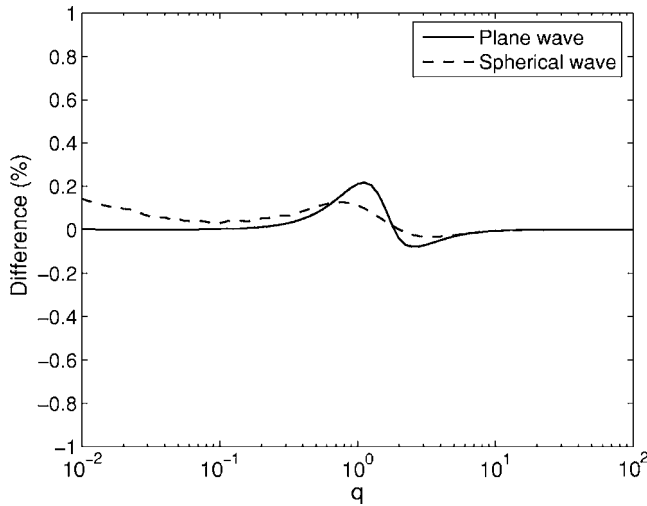


Fig. 4. Difference (%) between the exact (numerical) solution and the closed-form approximation of the aperture-averaged AOA variances for plane and spherical waves, respectively.

1. Small-Aperture and Large-Aperture Asymptotic Values
Now, we consider the two asymptotic cases $q \ll 1$ and $q \gg 1$ of the closed-form approximation of $\langle \bar{\theta}^2 \rangle_p$ for plane waves, Eq. (17), and we compare them with previous work.^{1,2,12}

For very small apertures, $q \ll 1$, the second term in the curly brackets of Eq. (17) is much smaller than 1 and negligible. Then, we have the asymptotic value,

$$\begin{aligned} \gamma_p(0) &= \frac{\sqrt{3}}{16} \Gamma\left(\frac{1}{6}\right) \Gamma\left(\frac{8}{3}\right) \left(\frac{\beta}{2}\right)^{-1/3} \\ &= \frac{\pi}{55} 2^{11/3} 3^{1/2} \frac{[\Gamma(2/3)]^2}{[\Gamma(5/6)]^4} = 1.419, \end{aligned} \quad (31)$$

where we have substituted β as given in Eq. (14). For very large apertures, $q \gg 1$, we can approximate several terms of $\gamma_p(q)$ as follows: $[1 + \pi^2 \beta^4 q^4 / 4]^{5/12} \approx (\pi \beta^2 q^2 / 2)^{5/6}$, $\arctan[2 / (\pi \beta^2 q^2)] \approx 2 / (\pi \beta^2 q^2)$, and $\sin[10 / (6 \pi \beta^2 q^2)] \approx 10 / (6 \pi \beta^2 q^2)$. Then, the second term in the curly brackets of Eq. (17) approaches 1, and we obtain the asymptotic value,

$$\gamma_p(\infty) = 2\gamma_p(0) = 2.838. \quad (32)$$

The numerical results for $\gamma_p(0)$ and $\gamma_p(\infty)$ are consistent with Tatarskii's numerical results (p. 289 in Ref. 2). Figure 3 shows that $\gamma_p(q)$ converges rapidly to $\gamma_p(\infty)$ for $q > 1$ and much less rapidly to $\gamma_p(0)$ for $q < 1$. While $[\gamma_p(\infty) - \gamma_p(q)] / \gamma_p(q)$ becomes smaller than 1% for $q > 1.65$, $[\gamma_p(q) - \gamma_p(0)] / \gamma_p(q)$ becomes smaller than 10% only for $q < 1.35 \times 10^{-3}$.

2. Intermediate Range

For finite $q < 1$ in Eq. (17), we can approximate: $[1 + \pi^2 \beta^4 q^4 / 4]^{5/12} \approx 1$ and $\arctan[2 / (\pi \beta^2 q^2)] \approx \pi/2$. Thus, $\gamma_p(q)$ is

$$\begin{aligned} \gamma_p(q) &\approx \gamma_p(0) \left[1 + \frac{6}{5} \left(\frac{\pi}{2}\right)^{1/6} \beta^{1/3} q^{1/3} \sin\left(\frac{5\pi}{12}\right) \right] \\ &= 1.419(1 + 1.006q^{1/3}). \end{aligned} \quad (33)$$

This approximation becomes invalid where $\gamma_p(q)$ exceeds the value of the large-aperture asymptote, which we know is $2\gamma_p(0)$. Therefore, approximation (33) becomes invalid beyond $q = 1.006^{-3}$, which is very close to 1. For larger q , the constant value $\gamma_p(\infty) = 2\gamma_p(0)$ approximates $\gamma_p(q)$ better. Hence,

$$\gamma_p(q) = \begin{cases} 1.419 + 1.4275q^{1/3} & \text{for } q \leq 1 \\ 2.838 & \text{for } q > 1 \end{cases}, \quad (34)$$

is a simple approximation that is very accurate far away from $q=1$ and that is still useful in the intermediate range as shown in Fig. 3. The difference between the asymptotic approximation (34) and the exact solution is 4% at $q = 1.006^{-3} = 0.9822$ and much smaller for q further away from 1.

C. Aperture-Averaged Angle-of-Arrival Variance for the Spherical Wave

Figure 5 shows three curves of $\gamma_s(q)$: a numerical solution of the integral (5) with the exact spherical-wave weighting function, $h_s(\kappa, u)$ given in Eq. (7), our closed-form approximation (with the Gaussian weighting function) as given in Eq. (27), and the asymptotic fit as given later in Eq. (39). The difference between the exact numerical solution and the closed-form approximation of $\langle \bar{\theta}^2 \rangle$ is shown in Fig. 4, and the maximum value of the difference is less than 0.2%, which is negligible.

1. Small-Aperture and Large-Aperture Asymptotic Values

As we did in Subsection 3.B for the plane-wave case, we now discuss the asymptotes of $\langle \bar{\theta}^2 \rangle_s$ for $q \ll 1$ and $q \gg 1$ in the spherical-wave case. For very small apertures, $q \ll 1$, we can simplify Eq. (27) by means of $[-2i / (\pi \beta^2 q^2)]^{-1/6} \approx 0$. Thus, we have the asymptotic value,

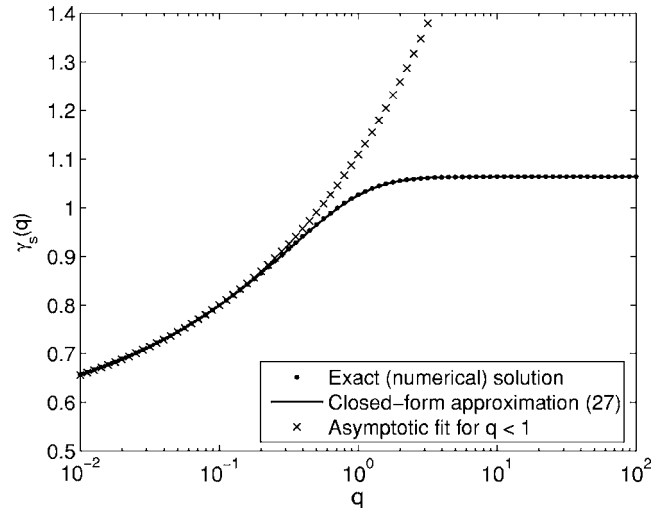


Fig. 5. Aperture-averaged AOA variance, normalized by $C^2 L D^{-1/3}$, versus q for a spherical wave. The dots are the exact (numerical) solution, the solid curve is the closed-form approximation (27), and the crosses are the asymptotic fit for $q < 1$.

$$\begin{aligned}\gamma_s(0) &= \frac{3\sqrt{3}}{8} \frac{\Gamma\left(\frac{1}{6}\right)\Gamma\left(\frac{8}{3}\right)\left(\frac{\beta}{2}\right)^{-1/3}}{16} \\ &= \frac{\pi}{55} 2^{2/3} 3^{3/2} \frac{[\Gamma(2/3)]^2}{[\Gamma(5/6)]^4} = 0.532,\end{aligned}\quad (35)$$

where $\beta=0.5216$. For very large apertures, $q \gg 1$, we can approximate the fourth argument of the hypergeometric function in Eq. (27) as $1-i\pi\beta^2q^2/2 \approx -i\pi\beta^2q^2=1/C_2$. Then, the hypergeometric function can be written as

$$\begin{aligned}{}_2F_1\left(\frac{1}{6}, \frac{17}{6}; \frac{23}{6}; \frac{1}{C_2}\right) &= \frac{\Gamma(23/6)\Gamma(16/6)}{\Gamma(17/6)\Gamma(22/6)} \left(-\frac{1}{C_2}\right)^{-1/6} \\ &\times {}_2F_1\left(\frac{1}{6}, -\frac{16}{6}; -\frac{10}{6}; C_2\right) \\ &+ \frac{\Gamma(23/6)\Gamma(-16/6)}{\Gamma(1/6)\Gamma(16/6)} \left(-\frac{1}{C_2}\right)^{-17/6} \\ &\times {}_2F_1\left(\frac{17}{6}, 0; \frac{22}{6}; C_2\right),\end{aligned}\quad (36)$$

where we have used Eq. (A7). Since we can approximate $C_2 \approx 0$ for $q \gg 1$, the first hypergeometric function on the right side of Eq. (36) can be approximated as 1. Then, after inserting into Eq. (27), we find the asymptotic value,

$$\gamma_s(\infty) = 2\gamma_s(0) = \frac{3}{8} 2.838 = 1.064,\quad (37)$$

which is consistent with previous work.⁴ Just as in the case of plane waves, $\langle \bar{\theta}^2 \rangle_s$ for very large apertures is twice the value of $\langle \bar{\theta}^2 \rangle_s$ for very small apertures. For both asymptotes, $\langle \bar{\theta}^2 \rangle_s$ is 3/8 times the value of $\langle \bar{\theta}^2 \rangle_p$. Figure 5 shows, like Fig. 3 in the plane-wave case, that $\gamma_s(q)$ converges rapidly to the asymptotic value $\gamma_s(\infty)=1.064$ for $q > 1$ and $\gamma_s(q)$ approaches $\gamma_s(0)=0.532$ much more gradually for $q < 1$, while $[\gamma_s(\infty) - \gamma_s(q)]/\gamma_s(q)$ becomes smaller than 1% for $q > 1.84$, $[\gamma_s(q) - \gamma_s(0)]/\gamma_s(q)$ becomes smaller than 10% only for $q < 1.068 \times 10^{-3}$.

2. Intermediate Range

For finite $q < 1$, we can approximate the hypergeometric function in Eq. (27) as ${}_2F_1(1/6, 17/6; 23/6; 1-i\pi\beta^2q^2/2) \approx {}_2F_1(1/6, 17/6; 23/6; 1)$. Evaluation by means of Eq. (A8) gives

$$\begin{aligned}\gamma_s(q) &\approx \gamma_s(0) \left[1 + \frac{6}{173} \operatorname{Re} \left\{ \left(-\frac{2i}{\pi\beta^2q^2} \right)^{-1/6} \right. \right. \\ &\quad \left. \left. \times {}_2F_1\left(\frac{1}{6}, \frac{17}{6}; \frac{23}{6}; 1\right) \right\} \right] \\ &= \gamma_s(0) \left[1 + 1.3279 \frac{6}{173} \left(\frac{\pi}{2}\right)^{1/6} \beta^{1/3} q^{1/3} \right] \\ &= 0.532(1 + 1.0847q^{1/3}).\end{aligned}\quad (38)$$

This approximation becomes invalid beyond $q=1.0847^{-3}$. For larger q , the constant value $\gamma_s(\infty)=2\gamma_s(0)$ approximates $\gamma_s(q)$ better. Therefore,

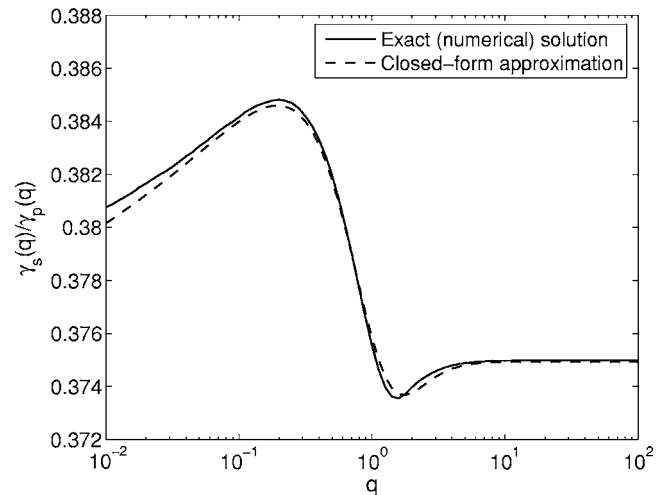


Fig. 6. Ratio between the aperture-averaged AOA variances for spherical and plane waves for the exact (numerical) solutions and the closed-form approximations, respectively.

$$\gamma_s(q) = \begin{cases} 0.532 + 0.577q^{1/3} & \text{for } q \leq 0.8, \\ 1.064 & \text{for } q > 0.8. \end{cases}\quad (39)$$

The difference between the asymptotic fit in Eq. (39) and the exact solution is $\sim 5\%$ at $q=1.0847^{-3}=0.7836$ and decreases quite rapidly for larger and smaller values of q .

D. Ratio of Spherical-Wave and Plane-Wave Aperture-Averaged Angle-of-Arrival Variance

Figure 6 shows $\gamma_s(q)/\gamma_p(q)$ as a function of q , that is, the ratio between variances for spherical and plane waves. For the asymptotic case $q \gg 1$, the ratio is $3/8=0.375$, which is known.¹² In the range of $0.2 < q < 1.8$, the ratio increases with decreasing q , since $\gamma_s(q)$ decreases more slowly than $\gamma_p(q)$ with decreasing q . The maximum of 0.385 occurs at $q \approx 0.2$. The minimum of 0.374 is reached at $q \approx 1.8$. While the ratio $\gamma_s(q)/\gamma_p(q)$ varies with q , it never deviates from 3/8 by more than 2.5%.

4. SUMMARY AND CONCLUSIONS

In this paper, we analyzed theoretically the variance $\langle \bar{\theta}^2 \rangle$ of aperture-averaged (assuming a circular aperture of diameter D) angle-of-arrival (AOA) fluctuations for plane and spherical waves of wavelength λ propagating along a path of length L through homogeneous and isotropic turbulence. We made the following assumptions: (1) the Rytov approximation is valid; (2) the refractive index spectrum is given by the inertial-range law $\Phi_n(\kappa) = 0.033C_n^2\kappa^{-11/3}$ for all wavenumbers that contribute to $\langle \bar{\theta}^2 \rangle$. To make the integrals for $\langle \bar{\theta}^2 \rangle$ more tractable, we approximated the Airy function in the integrals for $\langle \bar{\theta}^2 \rangle$ with a properly calibrated Gaussian function, $\exp[-(\beta a \kappa)^2]$, where $a=D/2$. We calibrated the width parameter β such that in the limit of very large Fresnel numbers $q=D/f = D/\sqrt{\lambda L}$ [i.e., in the geometrical-optics (GO) limit] the Airy-weighted $\langle \bar{\theta}^2 \rangle$ is equal to the Gaussian-weighted $\langle \bar{\theta}^2 \rangle$.

The main results are as follows:

1. For plane and spherical waves, the AOA variance can be written as $\langle \bar{\theta}^2 \rangle_p = \gamma_p(q) C_n^2 L D^{-1/3}$ and $\langle \bar{\theta} \rangle_s = \gamma_s(q) C_n^2 L D^{-1/3}$, respectively, where $\gamma_p(q)$ and $\gamma_s(q)$ are two different functions.

2. The width parameter turns out to be the same for plane waves and spherical waves: $\beta = 5^6 11^3 \Gamma^9(5/6) / [2^{16} 3^6 \Gamma^3(2/3)] = 0.5216$.

3. With β calibrated in the GO limit ($q \gg 1$), the Gaussian approximation of $\langle \bar{\theta}^2 \rangle$ is also exact in the point-aperture limit ($q \ll 1$).

4. For both plane and spherical waves, the GO-calibrated Gaussian approximation has an approximation error of less than 0.25% over the entire range of Fresnel numbers.

5. $\gamma_p(\infty) = 2\gamma_p(0)$ and $\gamma_s(\infty) = 2\gamma_s(0)$, that is, for both plane and spherical waves. The GO limit ($q \gg 1$) of $\langle \bar{\theta}^2 \rangle$ is twice the value of $\langle \bar{\theta}^2 \rangle$ in the point-aperture limit ($q \ll 1$).

6. $\gamma_p(\infty) = (\pi/55) 2^{14/3} 3^{1/2} [\Gamma^2(2/3)/\Gamma^4(5/6)] = 2.838$. The numerical result is consistent with Tatarskii's [Eq. (23a) on p. 289 in Ref. 2] result $\gamma_p(\infty) = 4 \times 0.71 = 2.84$.

7. The function $\gamma(q) - \gamma(0)$ closely follows a $q^{1/3}$ law for Fresnel numbers between 0 and ~ 1 , for both plane and spherical waves.

8. For plane waves, the GO limit of $\langle \bar{\theta}^2 \rangle_p$ is reached within 1% at $q = 1.65$. That is, for plane waves and aperture diameters larger than 1.65 Fresnel lengths, GO provides practically the same value for $\langle \bar{\theta}^2 \rangle_p$ as the Rytov approximation.

9. For spherical waves, the GO limit of $\langle \bar{\theta}^2 \rangle_s$ is reached within 1% at $q = 1.84$.

10. $\gamma_s/\gamma_p = 3/8$ both in the GO limit and in the point-aperture limit.

11. Over the entire range of Fresnel numbers, the largest deviation of γ_s/γ_p from its asymptotic value (3/8) is 2.5%.

APPENDIX A

This appendix lists a number of mathematical relationships that we used in our analysis.^{13,14} Equations (A1) to (A5) can be found in Ref. 13, and Eqs. (A6) to (A8) were taken from Ref. 14.

$$\int_0^\infty x^{-\mu} J_\nu^2(\alpha x) dx = \frac{\Gamma(\mu) \Gamma\left(\frac{2\nu+1-\mu}{2}\right)}{2^\mu \left[\Gamma\left(\frac{\mu+1}{2}\right)\right]^2 \Gamma\left(\frac{2\nu+1+\mu}{2}\right)} \alpha^{\mu-1} \quad (\text{A1})$$

for $0 < \mu < 2\nu+1$ and $\alpha > 0$.

$$\int_0^\infty x^\mu e^{-\alpha x^2} dx = \frac{1}{2} \Gamma\left(\frac{1+\mu}{2}\right) \alpha^{-(\mu+1)/2} \quad (\text{A2})$$

for $\alpha > 0$ and $\mu > -1$.

$$\int_0^\infty x^{\mu-1} e^{-\alpha x} \sin \delta x dx = \frac{\Gamma(\mu)}{(\alpha^2 + \delta^2)^{\mu+2}} \sin\left(\mu \arctan \frac{\delta}{\alpha}\right) \quad (\text{A3})$$

for $\text{Re}(\mu) > -1$ and $\text{Re}(\mu) > \text{Im}(|\delta|)$.

$$\int_0^1 dx x^m (C_1 x^2 - C_2 x)^n = \frac{(-C_2)^n}{n+m+1} {}_2F_1(-n, n+m+1; n+m+2; C_1/C_2), \quad (\text{A4})$$

$${}_2F_1(a, b; c; z) = \sum_{n=0}^\infty \frac{(a)_n (b)_n z^n}{(c)_n n!}, \quad (\text{A5})$$

where $(a)_n = a(a+1)(a+2)\cdots(a+n)$.

$$\begin{aligned} {}_2F_1(a, b; c; z) &= \frac{\Gamma(c)\Gamma(c-a-b)}{\Gamma(c-a)\Gamma(c-b)} {}_2F_1(a, b; a+b-c+1; 1-z) \\ &+ (1-z)^{c-a-b} \frac{\Gamma(c)\Gamma(a+b-c)}{\Gamma(a)\Gamma(b)} {}_2F_1(c-a, c-b; c-a-b+1; 1-z) \end{aligned} \quad (\text{A6})$$

for $|\arg(1-z)| < \pi$.

$$\begin{aligned} {}_2F_1(a, b; c; z) &= \frac{\Gamma(c)\Gamma(b-a)}{\Gamma(b)\Gamma(c-a)} (-z)^{-a} {}_2F_1(a, 1-c+a; 1-b \\ &+ a; 1/z) + \frac{\Gamma(c)\Gamma(a-b)}{\Gamma(a)\Gamma(c-b)} (-z)^{-b} {}_2F_1(b, 1-c \\ &+ b; 1-a+b; 1/z) \end{aligned} \quad (\text{A7})$$

for $|\arg(-z)| < \pi$.

$${}_2F_1(a, b; c; 1) = \frac{\Gamma(c)\Gamma(c-a-b)}{\Gamma(c-a)\Gamma(c-b)} \quad (\text{A8})$$

for $c \neq 0, -1, -2, \dots, \text{Re}(c-a-b) > 0$.

ACKNOWLEDGMENTS

This material is based upon work supported in part by the U.S. Army Research Laboratory and the U.S. Army Research Office under grant 49393-EV and by the National Science Foundation under grant ATM-0444688.

Y. Cheon's e-mail address is cheon@mirsl.ecs.umass.edu, and A. Muschinski's e-mail address is muschinski@ecs.umass.edu.

REFERENCES

1. V. I. Tatarskii, *Wave Propagation in a Turbulent Medium* (McGraw-Hill, 1961).
2. V. I. Tatarskii, *The Effects of the Turbulent Atmosphere on Wave Propagation* (Israel Program for Scientific Translation, 1971).
3. A. D. Wheelon, *Electromagnetic Scintillation. I. Geometrical Optics* (Cambridge U. Press, 2001).
4. A. S. Gurvich and M. A. Kallistratova, "Experimental study of the fluctuations in angle of incidence of a light beam under conditions of strong intensity fluctuations," *Radiophys. Quantum Electron.* **11**, 37-40 (1968).

5. J. H. Churnside and R. J. Lataitis, "Angle-of-arrival fluctuations of a reflected beam in atmospheric turbulence," *J. Opt. Soc. Am. A* **4**, 1264–1272 (1987).
6. J. H. Churnside, "Angle-of-arrival fluctuations of retroreflected light in the turbulent atmosphere," *J. Opt. Soc. Am. A* **6**, 275–279 (1989).
7. D. H. Tofsted, "Outer-scale effects on beam-wander and angle-of-arrival variances," *Appl. Opt.* **31**, 5865–5870 (1992).
8. R. Conan, J. Borgnino, A. Ziad, and F. Martin, "Analytical solution for the covariance and for the decorrelation time of the angle of arrival of a wave front corrugated by atmospheric turbulence," *J. Opt. Soc. Am. A* **17**, 1807–1818 (2000).
9. L. Andrews and R. Phillips, *Laser Beam Propagation through Random Media*, 2nd ed. (SPIE, 2005).
10. A. Ishimaru, *Wave Propagation and Scattering in Random Media* (Academic, 1978), Vol. 2.
11. J. Haddon and E. Vilar, "Scattering induced microwave scintillations from clear air and rain on earth space paths and the influence of antenna aperture," *IEEE Trans. Antennas Propag.* **AP-34**, 646–657 (1986).
12. A. S. Gurvich, M. A. Kallistratova, and N. S. Time, "Fluctuations in the parameters of a light wave from a laser during propagation in the atmosphere," *Radiophys. Quantum Electron.* **11**, 1360–1370 (1968).
13. I. S. Gradshteyn and I. M. Ryzhik, *Table of Integrals, Series, and Products*, 5th ed. (Academic, 1994).
14. M. Abramowitz and I. Stegun, eds., *Handbook of Mathematical Functions with Formulas, Graphs, and Mathematical Tables* (U.S. Department of Commerce, 1972).